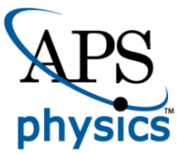

Distance-Dependent Sign Reversal in the Casimir-Lifshitz Torque

Priyadarshini Thiyam, Prachi Parashar, K. V. Shajesh, Oleksandr I. Malyi, Mathias Boström, Kimball A. Milton, Iver Brevik, and Clas Persson

Phys. Rev. Lett. **120**, 131601 — Published 26 March 2018

DOI: 10.1103/PhysRevLett.120.131601

Distance-dependent sign-reversal in the Casimir-Lifshitz torque

Priyadarshini Thiyam,[1,2,*] Prachi Parashar,[2,†] K. V. Shajesh,[3,2,‡] Oleksandr I. Malyi,[4,§] Mathias Boström,[2,4,¶] Kimball A. Milton,[5,**] Iver Brevik,[2,††] and Clas Persson[1,4,‡‡]

[1] *Department of Materials Science and Engineering, Royal Institute of Technology, SE-100 44 Stockholm, Sweden*
[2] *Department of Energy and Process Engineering, Norwegian University of Science and Technology, NO-7491 Trondheim, Norway*
[3] *Department of Physics, Southern Illinois University–Carbondale, Carbondale, Illinois 62901, USA*
[4] *Centre for Materials Science and Nanotechnology, Department of Physics, University of Oslo, P. O. Box 1048 Blindern, NO-0316 Oslo, Norway*
[5] *Homer L. Dodge Department of Physics and Astronomy, University of Oklahoma, Norman, Oklahoma 73019, USA*

The Casimir-Lifshitz torque between two biaxially polarizable anisotropic planar slabs is shown to exhibit a non-trivial sign-reversal in its rotational sense. The critical distance a_c between the slabs that marks this reversal is characterized by the frequency $\omega_c \sim c/2a_c$ at which the in-planar polarizabilities along the two principal axes are equal. The two materials seek to align their principal axes of polarizabilities in one direction below a_c, while above a_c their axes try to align rotated perpendicular relative to their previous minimum energy orientation. The sign-reversal disappears in the nonretarded limit. Our perturbative result, derived for the case when the differences in the relative polarizabilities are small, matches excellently with the exact theory for uniaxial materials. We illustrate our results for black phosphorus and phosphorene.

The Casimir-Lifshitz force [1] between neutral objects in the mesoscopic scales has been well established by the modern precision experiments [2]. This force is a manifestation of the quantum fluctuations in the electromagnetic fields that are confined by the boundaries, and is a retarded long-wavelength analogue of the van der Waals force when the finite speed of light c is taken into consideration. A conceptually related but a significantly challenging problem is that of the Casimir-Lifshitz torque, which arises when the rotational symmetry of the system is disrupted. The arduousness of calculating the Casimir-Lifshitz torque, including retardation effects, is demonstrated by the fact that the exact analytic evaluation of the torque between two uniaxially anisotropic semi-infinite half slabs by Barash [3] has never been reproduced by independent methods. A similar evaluation of the torque between two biaxially anisotropic materials is still lacking. Barash's calculation is the theoretical basis for the experimentally motivated papers in Refs. [4, 5]. The evaluation of the torque does become tractable in the nonretarded limit [6]; however, the Casimir-Lifshitz torque obtained in this way underestimates the magnitude even at 1 nm and fails to capture the non-trivial effects originating from retardation.

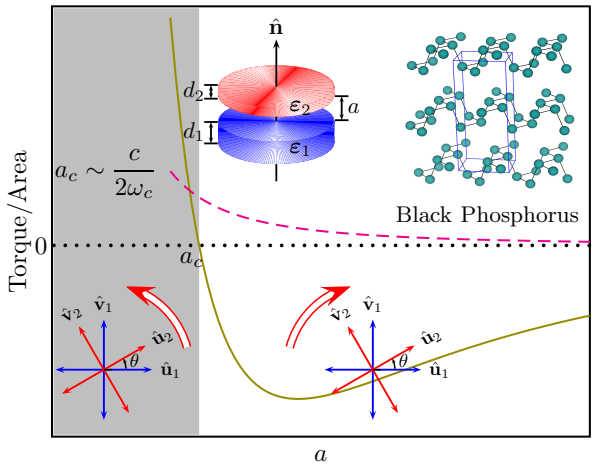

FIG. 1. Preview: The torque between two biaxially polarizable planar slabs as a function of the separation distance a. Our perturbation theory predicts that when the in-planar polarizabilities along the two principal axes of one of the materials are equal at a characteristic frequency ω_c, the torque may change sign at a critical distance a_c. Black phosphorus, whose crystalline structure is shown in the inset, and its monolayer phosphorene are such materials used in our analysis. The solid curve is a preview of our central result, shown here for the torque between two semi-infinite slabs of black phosphorus when the relative angle $\theta = \pi/4$. The dashed curve is the corresponding nonretarded limit.

In this article, we evaluate the torque between two parallel biaxially anisotropically polarizable slabs of finite thicknesses d_i, for $i = 1, 2$, separated by a distance a, as described in the inset of Fig. 1, in the retarded limit. We consider the case when the differences in the two in-planar polarizabilities, which are along the two in-planar principal axes, are small. We use a perturbative expansion in the parameter

$$\beta_i(\omega) = \frac{\varepsilon_i^u(\omega) - \varepsilon_i^v(\omega)}{\varepsilon_i^u(\omega) + \varepsilon_i^v(\omega)}, \tag{1}$$

that defines the degree of anisotropy in the polarizabilities of two media. Here, ω is the frequency associated

with the fluctuations of the fields. The leading order perturbative expression for the torque shows a simple linear dependence on the product $\beta_1\beta_2$, providing notable qualitative insight. In particular, it prompts us to predict a reversal in the direction of the torque as a function of the separation distance a. This change in the direction of the torque is marked by a critical distance $a_c \sim c/2\omega_c$, where ω_c is the corresponding characteristic frequency at which the perturbative parameter $\beta_i = 0$, i.e., the two in-planar polarizabilities of one media are equal. This prediction is motivated by the results in Ref. [7], which discusses similar effects in the context of Lifshitz pressure.

The reversal in the rotation of the torque as a function of separation distance has never been reported to our knowledge. The sign-reversal in the torque reported here is above and beyond the well understood change in the sign arising from the periodic oscillatory dependence in the angle θ [3–6]. We show that both black phosphorus (BP) and its two-dimensional (2D) monolayer phosphorene (2D-P) are suitable materials that permit $\beta_i(\omega_c) = 0$, characterized by crossings in the plots of their in-planar components of the dielectric functions with respect to frequency, as shown in Fig. 2. We verify and report our confirmation of the separation distance dependent sign-reversal of the torque experienced in slabs comprising of BP and 2D-P. The critical distance a_c is approximately 40 nm for BP and 2D-P, but with a little bit of material engineering it should be possible to construct materials that suit a specific need. In Fig. 1, we showcase the result for BP, where two slabs try to align their principal axes of polarizabilities in one direction below a_c, while above a_c they try to align their principal axes perpendicular relative to their previous minimum energy orientation. This sign-reversal behavior is absent in the corresponding nonretarded torque.

The major obstacle in calculating the torque is that the electromagnetic modes in the presence of a biaxially polarizable material do not separate into transverse electric (TE) and traverse magnetic (TM) modes. In our method, we circumvent this hindrance by choosing the system to be uniaxial in the absence of perturbation, $\beta_i = 0$ for all ω. For the setup shown in the inset of Fig. 1, we consider that the dielectric functions $\boldsymbol{\varepsilon}_i(\omega)$ of two nonmagnetic biaxially anisotropic slabs of thickness d_i are diagonal in the basis of their principal axes ($\hat{\mathbf{u}}_i$, $\hat{\mathbf{v}}_i$, $\hat{\mathbf{n}}$),

$$\boldsymbol{\varepsilon}_i(\omega) = \varepsilon_i^u(\omega)\,\hat{\mathbf{u}}_i\hat{\mathbf{u}}_i + \varepsilon_i^v(\omega)\,\hat{\mathbf{v}}_i\hat{\mathbf{v}}_i + \varepsilon_i^n(\omega)\,\hat{\mathbf{n}}\hat{\mathbf{n}}, \qquad (2)$$

where we chose one of the principal axis of each material to align normal to the slabs along $\hat{\mathbf{n}}$. We extend our perturbation methods in [8] to incorporate asymmetry in the polarization. We decompose

$$\boldsymbol{\varepsilon}_i(\omega) = \overline{\boldsymbol{\varepsilon}}_i(\omega) + \Delta\boldsymbol{\varepsilon}_i(\omega), \qquad (3)$$

where $\overline{\boldsymbol{\varepsilon}}_i(\omega)$ represents the uniaxial background

$$\overline{\boldsymbol{\varepsilon}}_i(\omega) = \varepsilon_i^{\perp}(\omega)\,(\hat{\mathbf{u}}_i\hat{\mathbf{u}}_i + \hat{\mathbf{v}}_i\hat{\mathbf{v}}_i) + \varepsilon_i^n(\omega)\,\hat{\mathbf{n}}\hat{\mathbf{n}} \qquad (4)$$

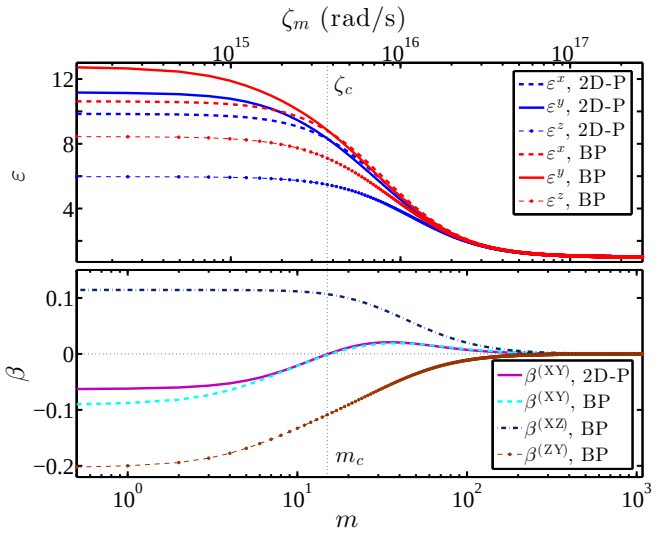

FIG. 2. Upper panel: Principal components of the dielectric tensors $\boldsymbol{\varepsilon}_i = \mathrm{diag}(\varepsilon_i^x, \varepsilon_i^y, \varepsilon_i^z)$ of BP and 2D-P, calculated using density functional theory (described in page 3). The imaginary Matsubara frequency ζ_m is obtained after making the Euclidean rotation; $\omega_m = i\zeta_m = i2\pi m k_B T/\hbar$. Components $\varepsilon_i^x = \varepsilon_i^y$ for both materials close to $\zeta_c \sim 4\times10^{15}$ rad/s. Lower panel: Perturbative parameter β_i for BP and 2D-P (shown for all three faces of BP crystal).

for which a closed form solution for the Green dyadic can be obtained. We define $\varepsilon_i^{\perp}(\omega) = (\varepsilon_i^u(\omega) + \varepsilon_i^v(\omega))/2$ so that the degree of anisotropy that characterizes the biaxial nature of the material is completely captured inside

$$\Delta\boldsymbol{\varepsilon}_i(\omega) = \left(\frac{\varepsilon_i^u(\omega) - \varepsilon_i^v(\omega)}{2}\right)(\hat{\mathbf{u}}_i\hat{\mathbf{u}}_i - \hat{\mathbf{v}}_i\hat{\mathbf{v}}_i). \qquad (5)$$

This particular choice renders $\mathrm{Tr}\,\Delta\boldsymbol{\varepsilon}_i(\omega) = 0$. The perturbative parameter in Eq. (1) can now be written as $\beta_i(\omega) = \Delta\varepsilon_i(\omega)/\varepsilon_i^{\perp}(\omega)$, which implies $\boldsymbol{\varepsilon}_i(\omega) = \overline{\boldsymbol{\varepsilon}}_i(\omega)(1 + \beta_i(\omega))$. It is easy to find materials with small β_i for all ω. For example, for the plane of 2D-P and the corresponding face of the BP crystal the magnitude of the static values of the perturbative parameter, $\beta_i(0)$, are approximately 0.06 and 0.09, respectively (see Fig. 2).

We evaluate the contribution to the interaction energy from the terms that are the first-order in the perturbative parameter β_i, separately, to be zero. Thus, the leading-order contribution to the interaction energy at finite temperature T is from the second-order term containing $\beta_1\beta_2$

$$\mathcal{E}^{(2)}(a,\theta) = -\frac{k_B T\cos 2\theta}{4\pi}{\sum_{m=0}^{\infty}}'\beta_1\beta_2\int_0^{\infty} k\,\mathrm{d}k\,\mathrm{Tr}(\widetilde{\boldsymbol{R}}_1\widetilde{\boldsymbol{R}}_2)e^{-2\kappa a}, \qquad (6)$$

where k_B is the Boltzmann constant, θ is the angle between the in-planar principal axes of the two materials shown in the co-ordinate system in Fig. 1, and k is the wave-vector perpendicular to $\hat{\mathbf{n}}$. The prime on the summation denotes that the zero frequency mode is taken

with half-weight. We define $\kappa = \sqrt{k^2 + \zeta_m^2/c^2}$, where ζ_m is defined in the caption of Fig. 2. The expression for the "reduced reflection" coefficient $\widetilde{\boldsymbol{R}}_i$ is given in the supplemental material [9]. We highlight that an exact expression for interaction energy between two biaxially polarizable materials, that includes retardation, remains an open problem–Barash's result is for uniaxial materials. Thus, our approximate expression for the interaction energy in Eq. (6) in the perturbative parameter $\beta_1\beta_2$, which is evaluated in the retarded limit, is a significant progress for the analysis of the interaction between biaxial materials. The details of our perturbation theory, which generalizes our earlier work [8], will be presented elsewhere.

The leading-order contribution to the torque per unit area on the dielectric slab is

$$\mathcal{T}^{(2)}(a,\theta) = -\frac{\partial}{\partial\theta}\mathcal{E}^{(2)}(a,\theta), \tag{7}$$

which replaces $\cos 2\theta$ by $2\sin 2\theta$ in Eq. (6). In the non-retarded limit, when we take $d_i \to \infty$ and set $\varepsilon^v = \varepsilon^n$, we reproduce Barash's uniaxial result in the corresponding weak limit. The 2θ dependence is a signature of bi-directional nature of fluctuation dependent polarizabilities. The dependence of torque on a is of the form $1/a^2$ times a function of d_i/a, which is usually monotonic. Here, we construct configurations of anisotropic materials that not only break away from the monotonous dependence on a but also change sign by carefully selecting configurations such that $\beta_i(i\zeta_c) = 0$ for at least one frequency. (Note that β_i will approach 0 at high frequencies.)

For two identical materials, the torque displays a monotonic behavior as a function of a because $\beta_1\beta_2 = \beta_1^2 \geq 0$ for all frequencies. However, for nonidentical materials, if $\beta = 0$ at a characteristic frequency ζ_c for one of the interacting materials (or β_i is zero for both the materials but at significantly different characteristic frequencies), then the Matsubara frequency modes above and below ζ_c will give contributions with opposite signs to the torque. The cancellation between the positive and negative contributions to the torque summed over all Matsubara frequencies in Eq. (6) will decide the overall sign of the torque at a fixed separation distance. The contributions from the higher Matsubara frequencies dominate at short separation distances while lower frequencies are more important at larger separation distances. These two competing effects create a scenario where the torque between two materials can reverse its rotational sense as a function of the separation distance. The sign-reversal of the torque is a generic behavior for any set of materials with the aforementioned material properties and is independent of the relative orientation θ.

The next-to-the-leading-order term $\mathcal{T}^{(4)}$ in the expression for the torque will contain $(\beta_1\beta_2)^2$ and $e^{-4\kappa a}$. Thus, this term is not only suppressed by the small magnitude of β_i but also subdued exponentially compared to the second-order term $\mathcal{T}^{(2)}$. Thus, the inclusion of this term cannot affect the sign-reversal behavior of the torque.

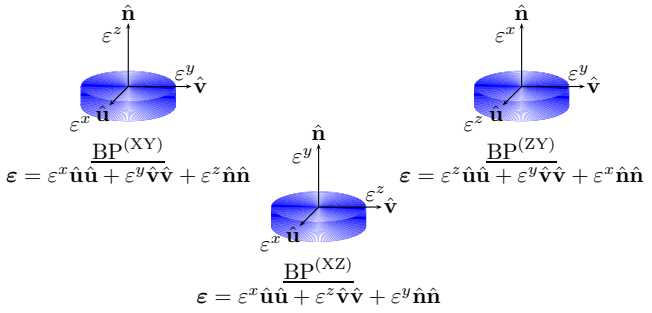

FIG. 3. Schematics for choices of interacting media for BP. We denote BP$^{(\mathrm{XY})}$ for the configuration when X-Y face of the BP aligns perpendicular to $\hat{\mathbf{n}}$. Similarly, BP$^{(\mathrm{XZ})}$ and BP$^{(\mathrm{ZY})}$ describe the configurations when X-Z and Y-Z faces of BP are set perpendicular to the $\hat{\mathbf{n}}$, respectively.

To illustrate the above mentioned change in the direction of the torque, we use BP and 2D-P, which are biaxially polarizable due to their puckered non-planar honeycomb structures [10]. The optical properties of BP and 2D-P are computed using the Vienna Ab-initio Simulation Package (VASP) [11]. The optB88-vdW functional [12] is used for structural relaxation while the revised Heyd-Scuseria-Ernzerhof (HSE) screened functional [13] is used for the dielectric function calculations. The computed band gap energies of BP and 2D-P are 0.38 and 1.52 eV, respectively, which are consistent with the previously reported results [14].(See supplemental material [9] for details.) The dielectric function data for black phosphorus calculated using density functional theory are comparable to the available low-frequency experimental data [15]. The data for phosphorene are not available to the best of our knowledge. (See supplemental material [9] for details.) Figure 2 displays the dielectric tensor components ε^x, ε^y, and ε^z, along the principal axes ($\hat{\mathbf{x}}_i$, $\hat{\mathbf{y}}_i$, $\hat{\mathbf{z}}$) of BP and 2D-P crystals as a function of ζ_m. The components ε^x and ε^y of the dielectric function of BP and 2D-P cross approximately at 4×10^{15} rad/s. The BP crystal has three faces–each with a different degree of anisotropy. In the Casimir-Lifshitz setup, shown in the inset of Fig. 1, we have the choice to align different faces perpendicular to $\hat{\mathbf{n}}$, as delineated in Fig. 3. The perturbative parameters corresponding to the three orientations of the BP crystal, and 2D-P, are presented in the lower panel of Fig. 2. Note that $\beta^{(\mathrm{XZ})}$ and $\beta^{(\mathrm{ZY})}$ for BP are never zero, which equips us with a suitable set of dielectric function for one of the interacting materials to test our theoretical predictions.

In the supplemental material [9], we show that the leading-order perturbative result, applied to the interaction between two uniaxial materials, excellently matches well below 5% with the exact theory. Thus, emboldened

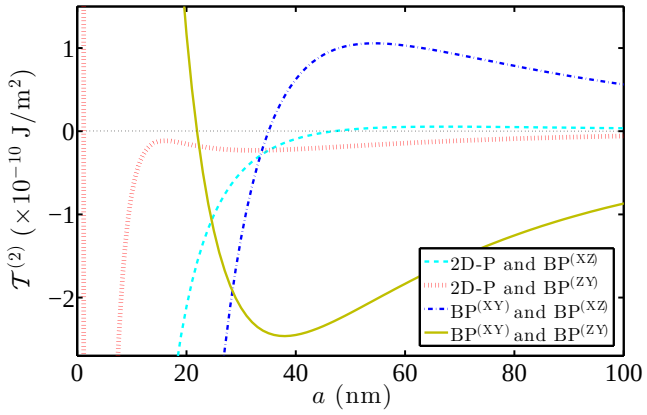

FIG. 4. Torque per unit area as a function of the separation distance a between different combinations of BP and 2D-P for $\theta = \pi/4$. The torque is not only nonmonotonic but also changes its sense of rotation as a function of a.

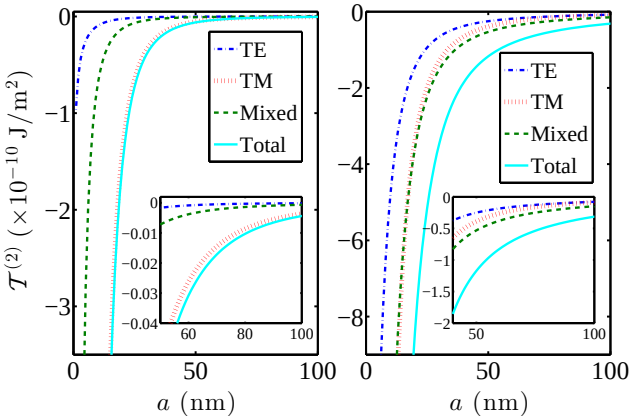

FIG. 5. Torque per unit area as a function of the separation distance a between two identical 2D-P layers (left panel) and two identical semi-infinite BP slabs (right panel). We show the TE, TM and mixed mode contributions, which have different hierarchical order in the two cases.

by the remarkable performance of the leading-order result, we proceed to test our main prediction of the sign-reversal of the torque. We evaluate the torque for the four different combinations of 2D-P and BP$^{(XY)}$ interacting with BP$^{(XZ)}$ and BP$^{(ZY)}$, which have a possibility of showing sign-reversal according to Eqs. (6) and (7). Our results for the leading-order torque as a function of the separation distance a are presented in Fig. 4. All the four cases show reversal in the direction of the torque at short separation distances ranging from 20-50 nm with the exception of interaction between 2D-P and BP$^{(ZY)}$ in which the torque changes sign at a very short distance but then shows multiple extrema as a function of a. This suggests that by manipulating the dielectric properties one could find multiple separation distances where the torque acting between two anisotropic materials may change its rotational sense for any arbitrary orientation between their in-planar principal axes. The results presented in the figure are for $\theta = \pi/4$. A different value of the relative orientation θ will change the magnitude and sign of the torque with a periodicity of $\sin 2\theta$.

Next, we investigate the scenario when the two interacting media are identical. As mentioned earlier, the torque is monotonic in this situation. Figure 5 shows the leading-order torque as a function of a for the interaction between two identical 2D-P in the left panel and between two semi-infinite slabs of BP$^{(XY)}$ in the right panel. In contrast to that of 2D materials, the magnitude of the torque between thick media is bigger by one to two orders of magnitudes. A similar monotonic behavior appears if one of the materials is 2D-P and the other material is the BP$^{(XY)}$, as $\beta_i = 0$ for both the materials at very close characteristic frequencies. Further, although the electromagnetic modes do not separate in biaxial systems, in our perturbation theory we can identify contributions to the torque from TE, TM, and a mixed mode, that depends on both TE and TM reflection coefficients defined for the uniaxial background of Eq. (4). The contributions from the TM mode to the torque dominates for small a of about 10 nm, followed by the mixed mode, with TE mode being negligible. All the modes begin to contribute comparably at large a of about 100 nm, but keep their hierarchical order for the case of interaction between two 2D-P layers. The interaction between two BP, on the other hand, presents a curious feature where the mixed mode over takes the TM mode at about 25 nm with TE mode also crossing over near 100 nm. From a fundamental point of view, this difference indicates a non-additive nature of the interlayer interaction in BP–also mentioned in Ref. [16] in the context of interlayer binding energy.

Before closing our discussion, we qualitatively comment on the feasibility of measuring the effects discussed here. The experimental verification of the Casimir-Lifshitz torque has remained elusive due to the smallness of the magnitude of the torque [17]. For a material slab with cross-sectional area of 100 μm^2, the torque is of the order of 10^{-20} Nm for BP and 2D-P, which is in accordance with the other calculations reported in the literature [4, 5, 18]. However, using an intervening liquid medium have shown an appreciable change in the magnitude of the torque [5, 19]. Other methods, like carrier injection to manipulate the dielectric functions, could provide enhancement in the torque. Newer experimental techniques as suggested in [20] could be explored. Our primary motivation, here, is to highlight the distance dependent sign-reversal in the Casimir-Lifshitz torque that should be kept in mind in the quest for an experimental verification. One may verify the existence of the torque, at least in principle, utilizing the sign-reversal of the torque. Assume, for instance, that the two planar materials at their initial positions are illuminated by

a laser beam from above, and the scattering pattern is observed. With the change of the separation distance between the slabs the torque will change its sense of rotation leading to a reorientation of the principal axes. Thus, the scattered radiation will have changed with the change of the separation distance. At least a qualitative change of the radiation pattern would be sufficient to verify the existence of the torque. The effect is analogus to Mie scattering from a dielectric sphere if subjected to slight surface deformations.

In conclusion, non-separability of TE and TM modes continues to be a hindrance in finding an exact solution for the torque between two biaxially anisotropic materials–Barash's solution in Ref. [3] was for a uniaxial material. However, we have developed a perturbative method that overcomes this shortcoming to an excellent accuracy. The change in the reversal of the torque highlighted here is expected to be prevalent in materials, and is an open door for device engineering.

ACKNOWLEDGEMENTS

We acknowledge support from the Research Council of Norway (Project No. 250346) and access to high-performance computing resources via SNIC and NOTUR. The work of KAM is supported in part by the US National Science Foundation (Grant No. 1707511).

* thiyam@kth.se
† prachi.parashar@ntnu.no
‡ kvshajesh@gmail.com
§ oleksandrmalyi@gmail.com
¶ Mathias.A.Bostrom@ntnu.no
** kmilton@ou.edu
†† iver.h.brevik@ntnu.no
‡‡ clas.persson@fys.uio.no

[1] H. B. G. Casimir, "On the attraction between two perfectly conducting plates," Kon. Ned. Akad. Wetensch. Proc. **51**, 793 (1948); E. M. Lifshitz, "The theory of molecular attractive forces between solids," Sov. Phys. JETP **2**, 73 (1956), [Translated from: Zh. Eksp. Teor. Fiz. **29**, 94 (1955)]; I. E. Dzyaloshinskii, E. M. Lifshitz, and L. P. Pitaevskii, "General theory of van der Waals' forces," Soviet Physics Uspekhi **4**, 153 (1961), [Translated from: Usp. Fiz. Nauk **73**, 381 (1961)].

[2] S. K. Lamoreaux, "Demonstration of the Casimir force in the 0.6 to 6 μm range," Phys. Rev. Lett. **78**, 5 (1997); "Erratum: Demonstration of the Casimir force in the 0.6 to 6 μm range [Phys. Rev. Lett. 78, 5 (1997)]," Phys. Rev. Lett. **81**, 5475 (1998); U. Mohideen and A. Roy, "Precision measurement of the Casimir force from 0.1 to 0.9 μm," Phys. Rev. Lett. **81**, 4549 (1998); H. B. Chan, V. A. Aksyuk, R. N. Kleiman, D. J. Bishop, and F. Capasso, "Nonlinear micromechanical Casimir oscillator," Phys. Rev. Lett. **87**, 211801 (2001); G. Bressi, G. Carugno, R. Onofrio, and G. Ruoso, "Measurement of the Casimir force between parallel metallic surfaces," Phys. Rev. Lett. **88**, 041804 (2002); F. Chen, U. Mohideen, G. L. Klimchitskaya, and V. M. Mostepanenko, "Demonstration of the lateral Casimir force," Phys. Rev. Lett. **88**, 101801 (2002); R. S. Decca, D. López, E. Fischbach, and D. E. Krause, "Measurement of the Casimir force between dissimilar metals," Phys. Rev. Lett. **91**, 050402 (2003); J. N. Munday, F. Capasso, and V. A. Parsegian, "Measured long-range repulsive Casimir-Lifshitz forces," Nature **457**, 170 (2009); L. Tang, M. Wang, C. Y. Ng, M. Nikolic, C. T. Chan, A. W. Rodriguez, and H. B. Chan, "Measurement of non-monotonic Casimir forces between silicon nanostructures," Nature Photonics **11**, 97 (2016).

[3] Yu. S. Barash, "Moment of van der Waals forces between anisotropic bodies," Radiophys. Quantum Electron. **21**, 1138 (1978), [Translated from: Izv. VUZ. Radiofizika **21**, 1637 (1978)].

[4] J. N. Munday, D. Iannuzzi, Y. Barash, and F. Capasso, "Torque on birefringent plates induced by quantum fluctuations," Phys. Rev. A **71**, 042102 (2005); "Erratum: Torque on birefrigent plates induced by quantum fluctuations [Phys. Rev. A 71, 042102 (2005)]," Phys. Rev. A **78**, 029906 (E) (2008); M. B. Romanowsky and F. Capasso, "Orientation-dependent Casimir force arising from highly anisotropic crystals: Application to $Bi_2Sr_2CaCu_2O_{8+\delta}$," Phys. Rev. A **78**, 042110 (2008); D. A. T. Somers and J. N. Munday, "Conditions for repulsive Casimir forces between identical birefringent materials," Phys. Rev. A **95**, 022509 (2017).

[5] D. A. T. Somers and J. N. Munday, "Casimir-Lifshitz torque enhancement by retardation and intervening dielectrics," Phys. Rev. Lett. **119**, 183001 (2017).

[6] V. A. Parsegian and G.H. Weiss, "Dielectric anisotropy and the van der Waals interaction between bulk media," J. Adhes. **3**, 259–267 (1972); B.-S. Lu and R. Podgornik, "van der Waals torque and force between dielectrically anisotropic layered media," J. Chem. Phys. **145**, 044707 (2016).

[7] M. Elbaum and M. Schick, "Application of the theory of dispersion forces to the surface melting of ice," Phys. Rev. Lett. **66**, 1713 (1991).

[8] I. Cavero-Peláez, K. A. Milton, P. Parashar, and K. V. Shajesh, "Noncontact gears. I. Next-to-leading order contribution to the lateral Casimir force between corrugated parallel plates," Phys. Rev. D **78**, 065018 (2008); "Noncontact gears. II. Casimir torque between concentric corrugated cylinders for the scalar case," Phys. Rev. D **78**, 065019 (2008); P. Parashar, K. A. Milton, I. Cavero-Peláez, and K. V. Shajesh, "Electromagnetic non-contact gears: prelude," in *Quantum Field Theory Under the Influence of External Conditions (QFEXT09)*, edited by K. A. Milton and M. Bordag (World Scientific, Oxford, UK, 2012) p. 48.

[9] See supplemental Material at [URL will be inserted by publisher] for the expression of the leading-order reduced "reflection coefficient", comparison with the exact uniaxial result, and details of the dielectric function calculation using density functional theory.

[10] H. Liu, A. T. Neal, Z. Zhu, Z. Luo, X. Xu, D. Tománek, and P. D. Ye, "Phosphorene: An unexplored 2D semiconductor with a high hole mobility," ACS Nano **8**, 4033 (2014).

[11] G. Kresse and J. Hafner, "Ab initio molecular dynamics for liquid metals," Phys. Rev. B **47**, 558–561 (1993).

[12] J. Klimeš, D. R. Bowler, and A. Michaelides, "Chemical accuracy for the van der Waals density functional," J. Phys. Condens. Matter **22**, 022201 (2010); "van der Waals density functionals applied to solids," Phys. Rev. B **83**, 195131 (2011).

[13] J. Heyd, G. E. Scuseria, and M. Ernzerhof, "Hybrid functionals based on a screened Coulomb potential," The Journal of Chemical Physics **118**, 8207–8215 (2003); A. V. Krukau, O. A. Vydrov, A. F. Izmaylov, and G. E. Scuseria, "Influence of the exchange screening parameter on the performance of screened hybrid functionals," J. Chem. Phys. **125**, 224106 (2006).

[14] O. I. Malyi, K. V. Sopiha, I. Radchenko, P. Wu, and C. Persson, "Tailoring electronic properties of multilayer phosphorene by siliconization," Phys. Chem. Chem. Phys. **20**, 2075–2083 (2018); X. Wang, A. M. Jones, K. L. Seyler, V. Tran, Y. Jia, H. Zhao, H. Wang, L. Yang, X. Xu, and F. Xia, "Highly anisotropic and robust excitons in monolayer black phosphorus," Nat. Nanotechnol. **10**, 517 (2015).

[15] H. Asahina, Y. Maruyama, and A. Morita, "Optical reflectivity and band structure of black phosphorus," Physica B+C **117-118**, 419–421 (1983); H. Asahina and A. Morita, "Band structure and optical properties of black phosphorus," Journal of Physics C: Solid State Physics **17**, 1839 (1984).

[16] L. Shulenburger, A.D. Baczewski, Z. Zhu, J. Guan, and D. Tománek, "The nature of the interlayer interaction in bulk and few-layer phosphorus," Nano Lett. **15**, 8170 (2015).

[17] F. Capasso and J. N. Munday, "Attractive and repulsive Casimir–Lifshitz forces, QED torques, and applications to nanomachines," in *Casimir Physics*, edited by D. Dalvit, P. Milonni, D. Roberts, and F. da Rosa (Springer, Berlin, Heidelberg, 2011) p. 249.

[18] J. Hu, *Ultrasonic Micro/Nano Manipulations: Principles and Examples* (World Scientific, Oxford, UK, 2014).

[19] T. A. Morgado, S. I. Maslovski, and M. G. Silveirinha, "Ultrahigh Casimir interaction torque in nanowire systems," Opt. Express **21**, 14943–14955 (2013).

[20] R. Guérout, C. Genet, A. Lambrecht, and S. Reynaud, "Casimir torque between nanostructured plates," EPL (Europhysics Letters) **111**, 44001 (2015); Z. Xu and T. Li, "Detecting Casimir torque with an optically levitated nanorod," Phys. Rev. A **96**, 033843 (2017).